Iranian Journal of Science and Technology, Transactions of Civil Engineering (2023) 47:987–1006
https://doi.org/10.1007/s40996-022-00920-y

RESEARCH PAPER

Performance-Based Seismic Design Optimization of Steel MRFs Under System and Component Constraints Using the IWSA Algorithm

Taha Bakhshpoori[1] · Arash Asadi Abadi[2] · Amirhossein Cheraghi[3] · Mohammad Farhadmanesh[3]

Received: 28 February 2022 / Accepted: 25 June 2022 / Published online: 16 July 2022

Abstract
Performance-based seismic design optimization (PBSDO), as a topic of growing interest, is applied to steel moment-resisting frames (MRFs) using the improved water strider algorithm (IWSA). Herein, PBSDO is carried out according to ASCE 41–17 provisions considering life safety and collapse prevention (CP) performance levels. IWSA is an enhanced version of the recently developed metaheuristic called the water strider algorithm (WSA), inspired from the life cycle of these insects. Two other metaheuristics, enhanced colliding bodies optimization (ECBO) and particle swarm optimization, are selected for the comparative study. In the current article, for the first time, all the essential constraints to fully simulate the practical PBSDO problem in accordance with the ASCE 41–17 for steel MRFs are considered for these newly developed algorithms, i.e., WSA and IWSA, to challenge them for a complex problem. Two MRFs with 9 and 24 discrete variables are studied here for this purpose. The constraints include non-seismic ones, i.e., geometry and strength (component level), as well as the seismic ones which consist of the inter-story drift ratio (system level), force-controlled and deformation-controlled members' acceptance criteria (component level). Furthermore, the strong column-weak beam (SCWB) criterion and plastic hinge distribution are investigated for the optimal designs. An efficient method is proposed to solve these complicated problems by which ECBO and IWSA could successfully solve both problems. The results demonstrate the predominance of the CP acceptance criteria constraints in the optimization and showcase the superiority or competitiveness of IWSA over the other three metaheuristics revealing its efficiency for complex structural optimization problems.

Keywords Structural optimization · Performance-based seismic design · Steel moment-resisting frames · Improved water strider algorithm

1 Introduction

Strong earthquakes such as USA Northridge (1994) and Japan Kobe (1995) provoked engineers and researchers to devise a new seismic design procedure for structures that was conventionally strength based. Although the casualties in these events were not significant, the damages incurred by structural components were enormous. This led the engineering community to develop the performance-based seismic design (PBSD) framework in which structures are designed to endure a specific damage level to satisfy the desired performance level of serviceability and strength in the face of future extreme events. The Federal Emergency Management Agency (FEMA) introduced several useful guidelines in PBSD; in this respect, one can refer to (FEMA-273 1997; FEMA-356 2000; FEMA-440 2005). Although these codes were originally meant to be used for evaluation and retrofit purposes, they opened a new horizon for designing of structures based on performance-based design (PBD) philosophy. Later, the ASCE 41–17, which is based on the aforementioned FEMA guidelines, opened a path to design new structures based on PBD concept other than evaluation and retrofit aims.

Many researchers have addressed the challenges of the PBD in recent years such as Saadat et al. 2014; Liu et al. 2013; Mansouri and Maheri 2019; and Khalilian et al. 2021.

✉ Taha Bakhshpoori
tbakhshpoori@guilan.ac.ir

[1] Faculty of Technology and Engineering, University of Guilan, East of Guilan, Roudsar, Guilan, Iran

[2] School of Civil Engineering, Iran University of Science and Technology, Narmak, Tehran, Iran

[3] Department of Civil and Environmental Engineering, The University of Utah, Salt Lake City, UT, USA

According to ASCE 41–17, for the risk category of II, the performance levels for designing new structures based on PBSD framework are as follows:

- Life safety (LS)
- Collapse prevention (CP)

At the LS level of performance, the structure is allowed to have damaged components, but it remains safe for occupants to evacuate the building. The CP performance level is defined as the state in which the structure has damaged components and retains no margin against collapse; however, it continues to tolerate gravity loads (ASCE41-17 2017).

In order to construct a cost-efficient structure, different earthquakes with various hazard levels are assumed to occur for a specific structure, and the structure is designed to have a particular performance level under those levels of an earthquake. The structure's performance level depends on the importance of the structure and the stakeholders' preference. The hazard level associated with the LS and CP performance levels for the new buildings in risk category of II is called BSE-1 N and BSE-2 N in ASCE 41–17, respectively. BSE-2 N denotes the basic safety earthquake-2 assumed as the ground shaking based on the risk-targeted maximum considered earthquake (MCE_R), and BSE-1 N shows the basic safety earthquake-1 or called the design earthquake (DE) taken as the two-thirds of the BSE-2 N at a site (ASCE7-16 2016).

In order to evaluate the seismic response of the structure, the nonlinear static procedure, also known as pushover analysis (POA), is often an attractive choice due to its simplicity and ability to identify component- and system-level deformation demands with accuracy comparable to dynamic analysis (Shayanfar et al. 2013). Under the FEMA-273, FEMA-356, and ASCE 41–17 approach, in which the acceptance criteria of a given performance level are determined based on component-level responses, the constraints are implemented such that each component's response is calculated and then compared to the allowable threshold.

The PBSD is a complex problem that entails adjusting many parameters; thus, it is difficult for designers to know whether the current design is the best or still there is a more desirable one. For this purpose, advancements in structural optimization have made it possible to move from traditional trial-and-error procedures toward an automatic approach (Fragiadakis and Lagaros 2011). Metaheuristic algorithms have gained growing popularity recently due to their efficiency in solving engineering problems in suitable time duration and acceptable accuracy for engineering objectives (Kaveh et al. 2018, 2013; Safari et al. 2021; Kaveh and Malakoutirad 2010; Makiabadi and Maheri 2021; Sedlar et al. 2021). Usually, the common characteristic of metaheuristic algorithms is the inspiration from natural or man-made phenomena. The water strider algorithm (WSA) is a new metaheuristic algorithm proposed by Kaveh and Dadras (2020). The viability of the algorithm in optimizing mathematical functions and size optimization of structures has formerly been investigated. Subsequently, Kaveh et al. proposed an improved water strider algorithm (IWSA) which uses opposition-based learning (OBL) and a mutation technique to enhance the standard WSA (Kaveh et al. 2020). The superiority of IWSA over WSA and many classical and well-established modern metaheuristics have already been demonstrated in their article.

The main purpose of structural optimization algorithms is to minimize the constructional cost of structures by building the lightest possible structure while satisfying several design constraints (Kaveh and Ghazaan 2018). In the framework of PBSD, structural optimization via metaheuristic algorithms has received considerable attention in recent years. Kaveh et al. used the ant colony optimization (ACO) algorithm for PBSD of steel moment-resisting frames (MRFs) and showed the superiority of ACO in comparison with the genetic algorithm (GA) for the discussed problems (Kaveh et al. 2010). Kaveh and Nasrollahi employed charged system search (CSS) algorithm for PBSD of steel frames and used POA based on semirigid connections and compared the results with the GA and ACO (Kaveh and Nasrollahi 2014). Gholizadeh used a modified firefly algorithm (MFA) and a new neural network for PBSD of steel structures (Gholizadeh 2015). They also used an improved quantum particle swarm optimization (Gholizadeh and Moghadas 2014) and Newton metaheuristic algorithm in this issue (Gholizadeh et al. 2020). Eftekhar et al. utilized a hybrid metaheuristic in this framework to obtain designs with lighter weights and higher convergence rate than all the existing results in the literature (Eftekhar et al. 2021). Degertekin et al. employed school-based optimization (SBO) for PBSD of steel frames (Degertekin et al. 2020) and compared the results with other metaheuristic algorithms, showing the outperformance of the SBO algorithm to others.

Although WSA and IWSA algorithms have shown promising results in size optimization of space structures such as double-layer barrel vaults (Kaveh and Dadras Eslamlou 2020; Kaveh et al. 2020), the literature review reveals that these algorithms have not been used in PBSD problems or a complex

engineering optimization problem so far. Furthermore, by studying the literature carefully, one realizes that the majority of articles have only considered system-level response such as inter-story drift ratio (IDR) for the entire optimization process, neglecting the component-level response; however, neglecting this fact is not allowed in FEMA-273, FEMA-356 or ASCE 41 since the acceptance criteria for the specified performance are measured based on component-level response. Moreover, it has been stated in Table C1-3 of FEMA-356 that the drift criterion is only a qualitative assessment of the performance of the structure. In this regard, there are a few studies in the literature taking into consideration the component-level response. For example, Wang et al. considered the strength and elements rotation ratio in the performance-based seismic design optimization (PBSDO) of two MRFs and conducted nonlinear time history analysis (Wang et al. 2019); nevertheless, they only deemed CP performance level for their optimization process and did not check geometric constraint (constructability) in the optimization. Fathali and Hoseini Vaez performed the optimum performance-based design of eccentrically braced frames (Fathali and Hoseini Vaez 2020), taking component- and system-level constraints into account. Fathizadeh et al. considered soil–structure effects on PBSDO of MRFs using an engineered cluster-based genetic algorithm (Fathizadeh et al. 2021). Hassanzadeh and Gholizadeh performed a collapse-performance-aided design of steel concentrically braced frames (Hassanzadeh and Gholizadeh 2019). Therefore, considering all the essential constraints to simulate a PBSD procedure according to ASCE 41 for MRFs have not been properly addressed in the literature yet. The strong capability of WSA and IWSA in search space exploration and achieving a suitable solution in a reasonable time inspired us to examine their ability on such problems as PBSDO. Thus, this study is herein proposed to investigate the efficiency of WSA and IWSA in solving a challenging and computationally demanding engineering problem, perform a comparative study on PBSDO problems, and extend their application. To the best of the authors' knowledge, this is the first time that steel MRFs are optimally designed using metaheuristic algorithms considering all of the essential constraints according to the ASCE 41–17 provisions.

To further investigate the competitiveness of the newly developed metaheuristic algorithms, particle swarm optimization (PSO) and enhanced colliding bodies optimization (ECBO) are utilized in this article to perform a comparative study. In fact, it has been demonstrated that PSO is the best performing algorithm in comparison with GA, ACO, and harmony search (HS) algorithms in the framework of PBSD of steel frames (Gholizadeh et al. 2013). Therefore, selecting PSO as the representative of a classical optimization method is justified. Moreover, ECBO has shown to be a robust optimization algorithm in structural optimization problems, including performance-based design optimization (Kaveh and Ilchi Ghazaan 2014; Kaveh and Farhadmanesh 2019; Fathali and Hoseini Vaez 2020). Thus, it is selected for a more comprehensive comparative study.

2 Performance-Based Seismic Design

The performance of structures is determined based on demand and capacity. The demand of the structure is defined given the expected earthquake, which is dependent on the level of the seismic hazard level, implying the rate of occurrence of the event. On the other hand, capacity is expressed by the design parameters of the structure, including the strength of elements, ductility, and proportioning. Thus, given the earthquake hazard level and the structures' capacity, performance levels are determined (Degertekin et al. 2020). In PBSD, a performance level is chosen for a specific hazard level. Commonly, for new buildings, the hazard level associated with 10 and 2% of probability of exceedance in 50 years has been respectively considered for the performance levels of LS and CP before the introduction of risk-targeted maximum considered earthquake (MCE_R) as new seismic design basis in ASCE 7. This earthquake is defined as the 1% probability of collapse of building in 50 years. Accordingly, the hazard level at the design earthquake (DE) is a uniform reduction of MCE_R. These earthquakes correspond to the mean return period of 475 (DE) and 2475 years (MCE_R) (ASCE41-17 2017).

In order to assess the seismic response of the structure, a nonlinear static procedure or POA is adopted in this article. Different methods have been proposed to conduct the POA recently (Shayanfar et al. 2019). Among the various methods, herein, the displacement coefficient method is employed (Hasan et al. 2002). In POA, the structure is subjected to increasing lateral loads until a predefined target displacement is reached. The monitored node for this displacement control analysis is taken as the center of mass for the roof story. The target displacement is calculated as follows according to ASCE41-17 2017:

$$\delta_t = C_0 C_1 C_2 S_a \frac{T_e^2}{4\pi^2} g \tag{1}$$

where C_0, C_1, and C_2 are the coefficients defined thoroughly in ASCE 41–17, S_a is the spectral response acceleration, g is

the gravity acceleration, and T_e is the effective fundamental period defined as:

$$T_e = T_i\sqrt{\frac{K_i}{K_e}} \tag{2}$$

where T_i is the fundamental elastic period, K_i is the elastic lateral stiffness, and K_e is the effective lateral stiffness. Since the determination of the target displacement is dependent on the bilinearization of the pushover curve, an iterative process might be necessary. In POA, the vertical distribution of the seismic forces is considered to be proportional to the shape of the fundamental mode:

$$C_{vx} = \frac{w_x h_x^k}{\sum_{i=1}^{ns} w_i h_i^k} \tag{3}$$

where C_{vx} represents the vertical distribution factor at each story level and w_x and w_i denote the portion of the total weight of the structure located at floor level x and i, respectively. h_x and h_i are the height from the base to floor level x and i, respectively. The parameter k is obtained by the following equation:

$$k = \begin{cases} 1 & T \le 0.5 \text{ sec} \\ 2 & T \ge 2.5 \text{ sec} \\ 0.5\,T + 0.75 & \text{else} \end{cases} \tag{4}$$

Additionally, spectral acceleration (S_a) can be calculated for the two performance levels as follows (ASCE41-17 2017):

$$\begin{aligned} &S_a = S_{XS}\left[\left(\frac{5}{B_1} - 2\right)\frac{T}{T_s} + 0.4\right] \; if \; 0 < T < T_0 \\ &S_{XS}/B_1 \; if \; T_0 < T < T_s \\ &S_{X1}/(B_1 T) \; if \; T_s < T < T_L \\ &T_L S_{X1}/(B_1 T^2) \; if \; T > T_L \end{aligned} \tag{5}$$

where $S_{X1} = F_v S_1$, $S_{XS} = F_a S_s$, $T_s = S_{X1}/S_{XS}$, $T_0 = 0.2T_s$, $B_1 = 4/[5.6 - \ln(100\beta)]$.

Table 1 Seismic design parameters of site class D, risk category II, and located in Los Angeles

Hazard level	F_a	F_v	$S_S(g)$	$S_1(g)$	$T_L(s)$
BSE-2 N (MCE_R)	1.2	1.7	1.974	0.703	8

In the above equations, T is the fundamental period of the structure, S_{XS} is the spectral response acceleration parameter at short periods, S_{X1} is the spectral response acceleration parameters at a 1-s period, F_a and F_v are the site coefficients, and β is the effective viscous damping ratio. A site with highly seismicity in Los Angeles (latitude: 34.05 longitude: − 118.24) is considered in this study. S_s and S_1 are determined based on the 11.4.2 provision of ASCE 7–16. Also, F_a and F_v are obtained from Table 11.4–1 and Table 11.4–2 of ASCE 7–16, respectively. These values are tabulated in Table 1. The damping ratio (β) of the structures is assumed to be 5%.

It is worth mentioning that S_{XS} and S_{X1} are the notation used in the code for the selected seismic hazard, either DE or MCE. The site parameters for the MCE (denoted by S_{MS} and S_{M1}) are determined first, and the corresponding values for the DE (denoted by S_{DS} and S_{D1}) are obtained by the following equations (ASCE7-16 2016):

$$\begin{cases} S_{DS} = \frac{2}{3}S_{MS} \\ S_{D1} = \frac{2}{3}S_{M1} \end{cases} \tag{6}$$

3 Metaheuristic Algorithms

In this research, four metaheuristics consisting of WSA, IWSA, PSO, and ECBO are employed for the optimization process. In the following subsections, these algorithms are briefly explained.

3.1 Water Strider Algorithm

The water strider algorithm is a novel population-based metaheuristic inspired by the life cycle of water striders that uses swarm intelligence. This algorithm employs territorial behavior, mating style, intelligent ripple communication, feeding mechanism, and succession of water strider insects to establish an efficient optimization algorithm that is competitive to many renowned classical optimization algorithms as well as the modern ones despite using simple mathematical equations. Water striders (WS) establish territories which are often inhabited by two WSs, one female and one male (keystone). Using a ripple communication system, the keystone sends ripples to the female WS to mate. The probability of attraction or repulsion from the female WS is supposed to be $p = 50\%$.

The next position of the keystone based on the reaction of the female is obtained as:

$$\begin{cases} \mathrm{WS}_i^{t+1} = \mathrm{WS}_i^t + \mathrm{R.rand}; \text{ if mating happens(with probability of } p) \\ \mathrm{WS}_i^{t+1} = \mathrm{WS}_i^t + R.(1 + \mathrm{rand}); \text{ otherwise} \end{cases} \tag{7}$$

The length of R equals the distance between the male and female WS:

$$R = \mathrm{WS}_F^{t-1} - \mathrm{WS}_i^{t-1} \tag{8}$$

where WS_i^t and WS_F^t represent the male and female WS positions in the t^{th} cycle, respectively. If the keystone's fitness is not improved in the new position, it moves towards the best candidate solution. There, the fitness value of the keystone is evaluated again. In case it decreases, a new WS will be generated to substitute it. These steps are repeated for other keystones as well. When all keystones' positions are updated, the WSs are assigned to new territories to start another loop. For a more comprehensive study of the steps of the algorithm, the reader can refer to (Kaveh and Dadras Eslamlou 2020).

3.2 Improved Water Strider Algorithm (IWSA)

There are two techniques incorporated in WSA to make it a more suitable global optimization algorithm. The first idea is based on OBL initially proposed by Tizhoosh for machine learning (Tizhoosh 2005), and the second idea is inspired by the mutation operator utilized in the GA.

Generalized space transformation search (GSTS) is utilized as the new formulation for OBL (Zhang and Jin 2020) to be applied to the initial population to provide a more promising search space for IWSA. The initial population plays an important role in the efficiency of the metaheuristic algorithms. In fact, random initialization might increase the probability of searching fruitless regions of search space. Utilizing OBL increases the ability of the optimization algorithms in terms of search space exploration and near-optimum exploitation of the search space. Moreover, in order to enhance the convergence speed, employing random numbers and their opposite is more beneficial than using pure randomness to generate initial estimates in the absence of prior knowledge about the solutions, as this method searches in two directions simultaneously (Rahnamayan et al. 2008).

To strengthen the exploration ability of the standard WSA algorithm, a mutation operator is added to enrich the algorithm to search more promising regions of the search space and assist it in escaping local optimums, which is an important issue in metaheuristics. The mutation technique is applied on the best-so-far solution in each iteration with a probability called *pro*.

Regarding the computational complexity of the IWSA, let C be the number of cycles that the algorithm needs to run, T the number of territories, and N the population size (number of water striders); then, the computational complexity of the IWSA can be calculated as follows: In the initialization part of the algorithm, the complexity of randomly initiating the population corresponds to $O(N)$ complexity and evaluating their opposites requires $O(N)$ complexity as well which leads to $O(2N)$ complexity for the initialization of IWSA. Then, for the updating part of the algorithm, the complexity is at least $O(CT)$ and at most $O(3CT)$ depending on the fitness of the keystone (similar to the standard WSA). Furthermore, after this updating process, the mutation operator is applied which corresponds to $O(0)$ or $O(CT)$ computational complexity based on the probability of the mutation. Therefore, the computational complexity of IWSA is between $O(2N + CT)$ and $O(2N + 4CT)$.

In this study, similar to the source article, the number of WSs and the territories are set as $nws = 50$ and $nt = 25$ for both WSA and IWSA algorithms.

3.3 Particle Swarm Optimization (PSO)

Particle swarm optimization (PSO) is one of the most well-known classical metaheuristics introduced by Kennedy and Eberhart. In PSO, the candidate solutions, so-called particles, are randomly initiated in the search space, and their positions are updated regarding the velocity of each particle. It is assumed that particles remember their best experienced position so far (xbest_i), and the whole swarm's best position (xgbest) as yet. Each particle's velocity is updated based on the following equation (Kennedy and Eberhart 1995):

$$v_{i,j}^{k+1} = w v_{i,j}^k + c_1 r_1 \left(\mathrm{xbest}_{i,j}^k - x_{i,j}^k \right) + c_2 r_2 \left(\mathrm{xgbest}_j^k - x_{i,j}^k \right) \tag{9}$$

where $x_{i,j}^k$ and $v_{i,j}^k$ represent the j^{th} component of the position and velocity vector of the i^{th} particle in the k^{th} iteration, respectively. r_1 and r_2 are two random numbers generated in [0,1]. c_1 and c_2 are constant numbers representing the cognitive and social behavior parameters, respectively. w is the inertia weight which is chosen to decrease linearly from 0.9

to 0.4 during the optimization (Eberhart and Shi 2000). The time step is considered to be unit. Thus, the particles' positions are updated as:

$$x_{i,j}^{k+1} = x_{i,j}^{k} + v_{i,j}^{k+1} \tag{10}$$

In this study, the internal parameters of PSO are set as: $c_1 = c_2 = 2$, and the population size is set to 50 as in WSA and IWSA algorithms.

3.4 Enhanced Colliding Bodies Optimization (ECBO)

Colliding bodies optimization (CBO) is a multi-agent algorithm that originated from collision laws in physics. In this algorithm, each candidate solution is called a colliding body (CB). The population is divided into two groups of stationary and moving groups, and the collision occurs between them to obtain a new position for each candidate solution. Enhanced colliding bodies optimization (ECBO) was introduced to improve the performance of CBO in terms of convergence speed and avoiding local optimums. In order to enhance the convergence rate, a memory is used to save some of the historically best solutions by defining a memory called colliding memory (CM). The CBs saved in CM are added to the population in each iteration, and the same number of current worst CBs is deleted. To help the CBO algorithm evade local optimums, a probability like *pro* is introduced, and for each CB, with a probability of *pro*, one of its components is regenerated randomly. Herein, the internal parameters of ECBO are selected as: Populationsize = 50, $pro = 0.3$. For a more comprehensive explanation of the ECBO algorithm, the reader may refer to Kaveh and Ilchi Ghazaan 2014.

4 Performance-Based Seismic Design Optimization Procedure

In this section, the formulation for PBSDO is presented. The optimization procedure can be mathematically expressed as follows:

Find $\{X\} = [x_1, x_2, \ldots, x_{ng}]$

$$\text{to minimize} W(\{X\}) = \sum_{i=1}^{ng} x_i \sum_{j=1}^{nm(i)} \rho_j L_j \tag{11}$$

$$\text{subjected to:} \begin{cases} g_j(\{X\}) \le 0, j = 1, 2, \ldots, nc \\ x_{i\min} \le x_i \le x_{i\max} \end{cases}$$

where $\{X\}$ is the design variables vector chosen from the 267 wide flange sections provided in the AISC database. The sections are sorted based on their cross-section areas in the first place and for equal cross-sectional areas, the moment of inertia (I_x) sorts the list. $W(\{X\})$ represents the weight of the structure, *ng* is the number of design groups, $nm(i)$ is the number of members associated with the *ith* group, and ρ_j and L_j indicate the density of the material and the length of the *jth* member, respectively. $g_j(\{X\})$ represents the design constraints of the problem specified by the standard codes, and *nc* is the number of constraints. x_{imin} and x_{imax} are the lower bound and the upper bound of the variable x_i, respectively. For constraints handling, the well-known penalty approach is utilized here. Thus, the objective function is redefined as follows:

$$P(\{X\}) = (1 + \alpha G) \times W(\{X\}) \tag{12}$$

where $P(\{X\})$ is the penalized weight or objective function to be minimized and α represents the penalty coefficient which is set as a large number (equal to 100 herein as being suitable for the problems). G denotes the sum of the violations of the design constraints and is calculated as follows:

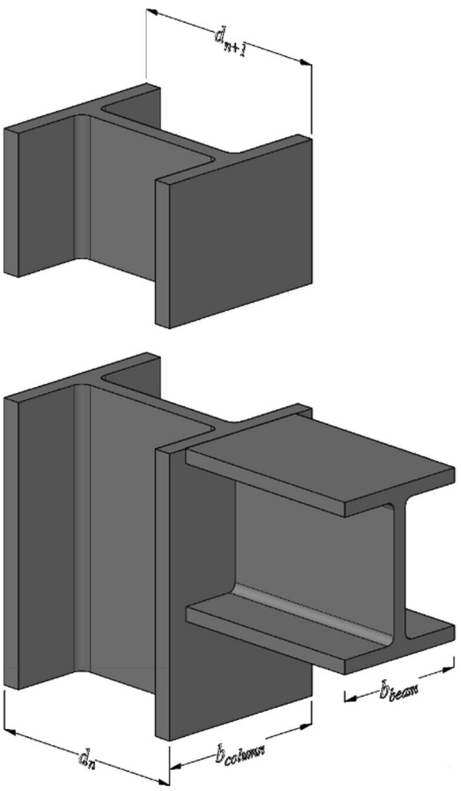

Fig. 1 Geometry of frames' connections for constructability

$$G = \sum_{i=1}^{n} \max\left(g_i, 0\right) \tag{13}$$

where g_i is the *ith* constraint considered and n is the number of constraints of the problem.

5 Optimization Constraints

To ensure that the desired design is obtained, five types of constraints consisting of seismic and non-seismic ones are taken into account during the optimization.

5.1 Non-Seismic Constraints

Non-seismic constraints include geometric and strength constraints that are checked here before conducting the POA.

5.1.1 Geometric Constraint

In order to make the structure constructable, certain geometric constraints must be met during the optimization process as seen in Fig. 1. Therefore, Eq. (14) is checked in each node to make sure the beams and columns dimensions are compatible. In the following equations, $(b_{\text{beam}})_i$ and $(b_{\text{column}})_i$ are the flange width of the i^{th} beam and column, respectively, and n_{BC} is the number of beam-column connections. $(d_{n+1})_j$ and $(d_n)_j$ are the depth of the j^{th} column at the $(n+1)^{th}$ and n^{th} story. In addition, n_{CC} and n_s show the number of column-column connections and the number of stories in the structure, respectively.

$$g_1 = \begin{cases} (b_{\text{beam}})_i/(b_{\text{column}})_i - 1 \le 0; i = 1, 2, \ldots, n_{\text{BC}} \\ (d_{n+1})_j/(d_n)_j - 1 \le 0; j = 1, 2, \ldots, n_{\text{CC}}; s = 1, 2, \ldots, n_s - 1 \end{cases} \tag{14}$$

5.1.2 Strength Constraint

In terms of strength constraint, all of the structural members are assessed whether they sustain the following gravity load combination (ASCE7-16 2016):

$$Q_G^{\text{type1}} = 1.2DL + 1.6LL \tag{15}$$

where DL and LL denote the dead load and live load, respectively ($DL = 2500kgf/m, LL = 1000kgf/m$). The strength constraint is expressed by flexural moment-axial force interaction relation according to (AISC360-16 2016):

$$g_2 = \begin{cases} \frac{P_u}{2\varphi_c P_n} + \left(\frac{M_{ux}}{\varphi_b M_{nx}} + \frac{M_{uy}}{\varphi_b M_{ny}}\right) - 1.0 \le 0.0 if \frac{P_u}{\varphi_c P_n} < 0.2 \\ \frac{P_u}{\varphi_c P_n} + \frac{8}{9}\left(\frac{M_{ux}}{\varphi_b M_{nx}} + \frac{M_{uy}}{\varphi_b M_{ny}}\right) - 1.0 \le 0.0 if \frac{P_u}{\varphi_c P_n} \ge 0.2 \end{cases} \tag{16}$$

where M_{ux} and M_{uy} are the required flexural strength in respect to the strong and weak axes, respectively; M_{nx} and M_{ny} are the nominal flexural strength in respect to the strong and weak axes, respectively; P_u and P_n denote the required and nominal axial strength, respectively, φ_c is the resistance factor ($\varphi_c = 0.9$ for tension or compression), and φ_b is the flexural resistance factor equal to 0.9.

5.2 Seismic Constraints

According to ASCE 41–17, the gravity loads assigned to the structure before starting the POA are considered to be:

$$Q_G^{\text{type2}} = DL + LL \tag{17}$$

where DL is the dead load and LL is the effective live load equal to 25% of unreduced design live load.

5.2.1 Inter-Story Drift Ratio Constraint (IDR)

The IDR constraint is calculated for each performance level by the following equation:

$$g_3 = \frac{d_k^i}{d_{all}^i} - 1 \le 0.0 i = \text{LS, CP}; k = 1, 2, \ldots, \text{ns} \tag{18}$$

where ns indicates the number of stories, d_k^i denotes the IDR of the kth story for performance level of i, and d_{all}^i is its allowable value. The allowable IDRs are considered to be 2.5% and 5% for the LS and CP performance level, respectively, as recommended by FEMA-365 2000.

5.2.2 Deformation-Controlled Members Constraints

Plastic hinge distribution plays an important role in performance-based design by showing the element-level behavior of structures. In addition, the element-level performance can predict collapse mechanisms and the formation

Table 2 Acceptance criteria for nonlinear procedures

	Modeling parameters	Acceptance criteria (plastic hinge rotation (Rad))	
		LS	CP
Beams	$\frac{b_f}{2t_f} \le o.30\sqrt{\frac{E}{F_{ye}}} and \frac{h}{t_w} \le 2.45\sqrt{\frac{E}{F_{ye}}}$	$9\theta_y$	$11\theta_y$
Columns in compression	$\frac{b_f}{2t_f} \le o.30\sqrt{\frac{E}{F_{ye}}} and$	$0.75b$	b
	$for \ \frac{P_G}{P_{ye}} < 0.2 \frac{h}{t_w} \le 2.45\sqrt{\frac{E}{F_{ye}}}(1-0.71\frac{P_G}{P_{ye}})$		
	$for \ \frac{P_G}{P_{ye}} \ge 0.2 \frac{h}{t_w} \le 0.77\sqrt{\frac{E}{F_{ye}}}(2.93-\frac{P_G}{P_{ye}}) \le 1.49\sqrt{\frac{E}{F_{ye}}}$		
	$a = 0.8\left(1-\frac{P_G}{P_{ye}}\right)^{2.2}(0.1\frac{L}{r_y}+0.8\frac{h}{t_w})^{-1} - 0.0035 \ge 0$		
	$b = 7.4\left(1-\frac{P_G}{P_{ye}}\right)^{2.3}(0.5\frac{L}{r_y}+2.9\frac{h}{t_w})^{-1} - 0.006 \ge 0$		
Columns in tension	$for \ \frac{\lvert P_G\rvert}{P_{ye}} < 0.2$	$9\theta_y$	$11\theta_y$
	$for \ \frac{\lvert P_G\rvert}{P_{ye}} \ge 0.2$	a	b
	$a = 13.5\left(1-5/3\frac{\lvert P_G\rvert}{P_{ye}}\right)\theta_y \ge 0$		
	$b = 16.5\left(1-5/3\frac{\lvert P_G\rvert}{P_{ye}}\right)\theta_y \ge 0$		

of soft stories during extreme events. Herein, the plastic hinge growth of the frames of this study has been investigated for each defined performance level. The criteria by which the performance levels are determined are in accordance with ASCE 41–17 provisions for structural steel components. According to this standard, members that are able to show inelastic behavior are classified as deformation-controlled and their rotation must satisfy the following relation:

$$g_4 = \frac{\theta_j^i}{\theta_{\mathrm{AC},j}^i} - 1 \le 0; j = 1, 2, \ldots, \mathrm{ne} i = \mathrm{LS}, \mathrm{CP} \tag{19}$$

In the above equation, θ_j^i and $\theta_{\mathrm{AC},j}^i$ denote the absolute value of the rotation of the j^{th} plastic hinge, and its acceptance criterion for the i^{th} performance level, respectively. Considering the compactness of the sections used herein, the acceptance criteria for this study are provided in Table 2 where P_G represents the axial force component of the gravity load obtained by exerting Q_G^{type2}, and the yield rotation of the members, θ_y, is calculated by the following formulas (ASCE41-17 2017):

$$\begin{cases} \theta_y = \dfrac{M_{pe}L(1+\eta)}{6EI} \text{ for beams} \\ \theta_y = \dfrac{M_{pce}L(1+\eta)}{6\left(\tau_b E\right)I} \text{ for columns} \end{cases} \tag{20}$$

where

$$\eta = \frac{12EI}{L^2 GA_s}$$

$$\begin{cases} \tau_b = 1.0 \, for \, \dfrac{|P|}{P_{ye}} \le 0.5 \\ \dfrac{4|P|}{P_{ye}}\left(1-\dfrac{|P|}{P_{ye}}\right) for \, \dfrac{|P|}{P_{ye}} > 0.5 \end{cases}$$

$$\begin{cases} M_{CE} = M_{pe} \text{ for beams} \\ M_{CE} = M_{pce} = \begin{cases} M_{pe}\left(1-\dfrac{|P|}{2P_{ye}}\right) for \, \dfrac{|P|}{P_{ye}} < 0.2 \\ M_{pe}\dfrac{9}{8}\left(1-\dfrac{|P|}{P_{ye}}\right) for \, \dfrac{|P|}{P_{ye}} \ge 0.2 \text{ for columns} \end{cases} \end{cases} \tag{21}$$

In the above equations, E is the modulus of elasticity, F_{ye} is the expected yield stress, L denotes the length of the beam or column members, M_{CE} is the expected flexural strength of the member, I is the moment of inertia of the beam or column members, G is the shear modulus, A_s is the effective shear area of the cross section, M_{pe} is the expected plastic moment capacity of the section about the bending axis calculated as $M_{pe} = ZF_{ye}$ (Z denotes the plastic section modulus), P is the axial force in the member at the target displacement, and P_{ye} shows the expected axial yield force of the member ($= A_g F_{ye}$). Herein, the value of η is set equal to zero as permitted by the code for the sections and mathematical modeling of this study. Moreover, the expected values of the parameters are set equal to their original values.

5.2.3 Force-Controlled Members Constraints

According to ASCE 41–17 and ignoring the lateral-torsional buckling, the columns that their modeling parameter, a, as provided in Table 2, is equal to zero or where $P_G/P_{ye} > 0.6$, shall remain elastic for flexure, and are not expected to develop ductile behavior. Hence, they are considered force-controlled in this study. These columns shall also satisfy the following constraint in addition to the criteria of Table 2:

$$g_5 = \begin{cases} \dfrac{|P|}{2P_{yLB}} + \dfrac{M_x}{M_{pLBx}} + \dfrac{M_y}{M_{pLBy}} - 1 \le 0 \; for \; \dfrac{|P|}{P_{yLB}} > 0.2 \\ \dfrac{|P|}{P_{yLB}} + \dfrac{8}{9}\left(\dfrac{M_x}{M_{pLBx}} + \dfrac{M_y}{M_{pLBy}}\right) - 1 \le 0 \; for \; \dfrac{|P|}{P_{yLB}} \ge 0.2 \end{cases} \tag{22}$$

where P denotes the required axial force of the column, M_x and M_y are, respectively, the required bending moments about the x- and y-axis, and all calculated at the target displacement. P_{yLB} represents the lower bound of the axial yield strength of the member ($= A_g F_{yLB}$), M_{pLBx} and M_{pLBy} are the lower bound plastic moment capacity of the section about the x- and y-axis, respectively. M_{pLBx} and M_{pLBy} can be obtained using Eq. (21). Also, the lower bound values of the parameters are set to their original values in the article.

To reduce the computational cost due to excessive numbers of pushover analyses, firstly, the non-seismic constraints are checked, and then, in case of zero penalty, the algorithm proceeds to assess the seismic constraints. Also, it is noteworthy to mention that the candidate solutions are rejected if they do not satisfy the non-seismic constraints by applying a large penalty coefficient ($\alpha = 10^9$); otherwise, POA is performed to determine the IDR and deformation or force-controlled members' constraints. The proposed method's flowchart is depicted in Fig. 2.

6 Simulation

Two structures consisting of 6- and 12-story MRFs are studied here for PBSDO. Considering the practical aspects of the construction and the symmetry of the structures, the frames are grouped into 9 and 24 design variables, as shown in Fig. 3. Since the objective function evaluation is costly and time-consuming, the MaxNFE of 20,000 is considered the algorithms' termination criterion for the two frames. In each iteration, a vector of design variables, herein columns and beams' sections, is returned to OpenSees (Mazzoni et al. 2006) so as to calculate the model response under lateral loadings that are incremented to reach the target displacement. To this end, the distributed plasticity simulation has been adopted, and the fiber model is employed to simulate the nonlinear behavior. The *bilinear* constitutive model is then used for nonlinear behavior via *steel01* uniaxial material with a 3% strain-hardening ratio. The element *nonlinearBeamColumn* is utilized with the intended w-sections assigned; also, the number of integration points is assumed to be 7 along each element. The connections of all the frames are assumed to be fully restrained, and for the sake of reducing the computation burden, deformation of panel zones and nonlinear behavior of connections have been idealized using *equalDof* command. In order for diaphragms, herein beams, to simulate rigid behavior, a constraint is employed in the horizontal direction between beams' nodes so that rigid diaphragm behavior realizes. After computing the eigenvalues of the model and deriving the fundamental period, gravity analysis is done. Afterwards, POA is applied to compute the models' seismic constraints for a specific target displacement determined according to the intended performance level.

Mechanical properties of the steel are assumed as shown in Table 3:

The estimated coefficients for the target displacement for each frame are provided in Table 4. It is worth mentioning that $\boldsymbol{C}_0$ was calculated using Table 7–5 of the ASCE 41–17, and the other two coefficients were approximately estimated by a process of trial and error for these structures.

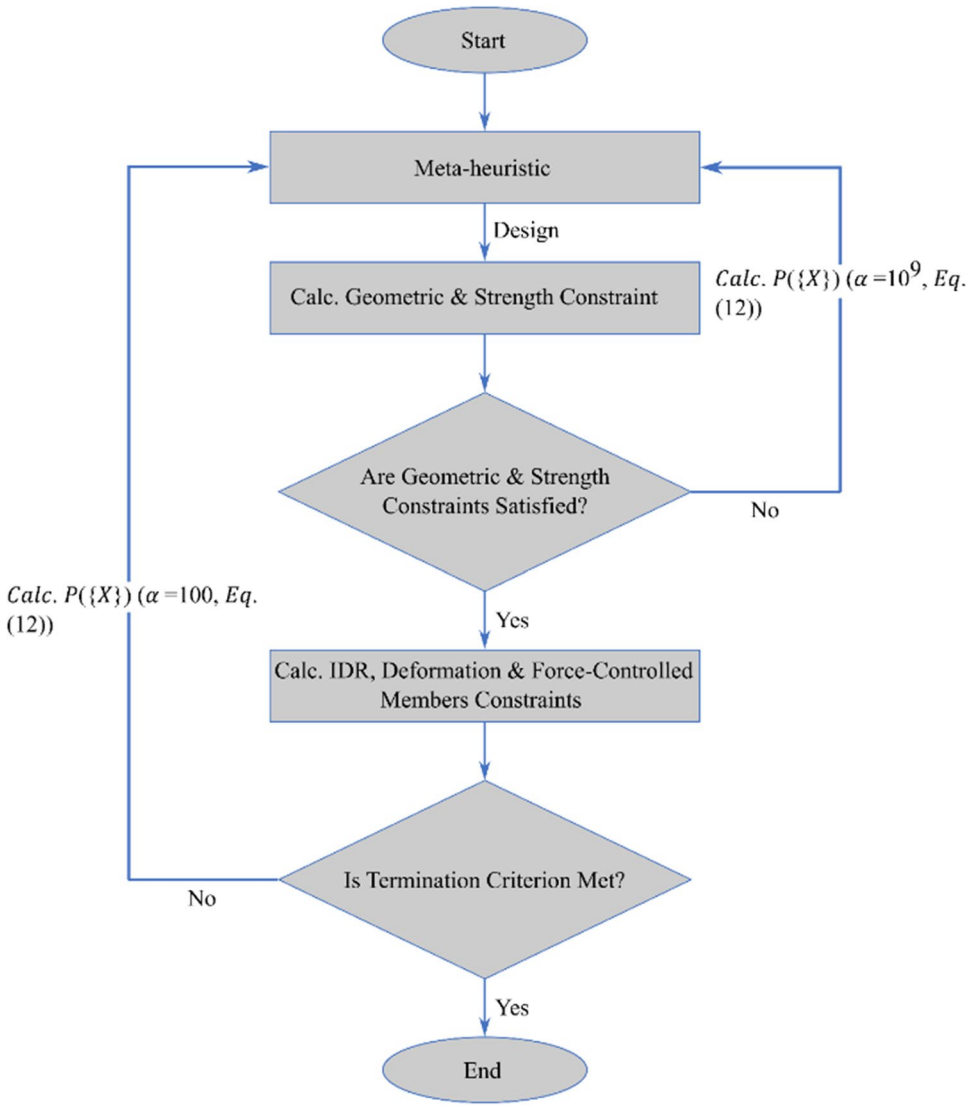

Fig. 2 Flowchart of the proposed method

7 Results and Discussions

In this section, the results of designing the two frames by the algorithms are discussed. The 1st example is run 10 times independently, and 6 independent runs were carried out for the 2nd one to provide reasonable statistical results.

7.1 6-story Frame

The first example is a 3-bay, 6-story frame depicted in Fig. 3a. The design variables include 6 groups for columns and 3 groups for beams as demonstrated in Fig. 3a. The best designs achieved by the algorithms without any constraint violations are shown in Table 5. As can be seen, the best design of IWSA (bolded in the table) is 4.2 and 10% better than its standard version and PSO, respectively. In addition, it is 3.5% lighter than the best result of ECBO. For a better insight into the performance of the three algorithms in the ten runs, the average optimized weight is also provided in Table 5. As shown, the average optimized weight of IWSA is 21171.56 kg which is 6.2% and 9.8% lighter than WSA and PSO, respectively. This shows the superiority of the IWSA over its standard version and PSO in the optimization

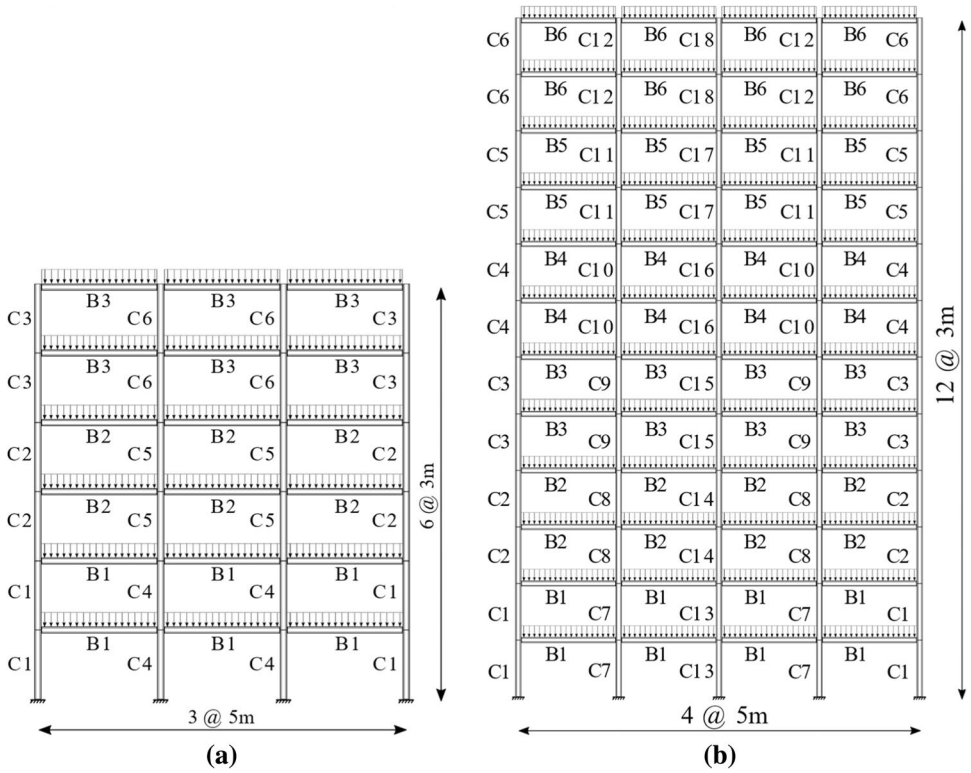

Fig. 3 Schematic of the two frames considered for PBSDO; **a** the 6-story frame **b** the 12-story frame

Table 3 Mechanical properties of the considered steel

Young's modulus	Yield stress	Density	Poisson's ratio
210*GPa*	235*MPa*	7850kg/m^3	0.3

Table 4 Coefficients for calculating the target displacement

	6-story frame	12-story frame
C_0	1.42	1.5
C_1	1	1
C_2	1	1

process. However, the mean result of ECBO is slightly better than IWSA. This number, along with a low value of the standard deviation of ECBO, shows the satisfactory performance of this metaheuristic in the ten independent runs.

The convergence curves for the best design of the algorithms are shown in Fig. 4. It can be seen that the IWSA has the highest convergence rate in comparison with the other metaheuristics. It is worth mentioning that despite beginning the optimization with a similar initial solution to the WSA, the higher convergence rate of IWSA is evident in later stages of the optimization. This demonstrates that the strategies utilized in IWSA were instrumental in enhancing the convergence speed of the algorithm.

Table 5 The best design achieved by the algorithms for the 6-story frame

Groups	PSO	ECBO	WSA	IWSA
C1	W40×149	W44×262	W30×124	W30×99
C2	W24×76	W18×76	W30×90	W30×90
C3	W16×100	W12×40	W18×50	W24×68
C4	W33×152	W33×118	W27×178	W30×116
C5	W27×114	W30×99	W27×102	W30×99
C6	W24×76	W30×90	W24×76	W18×60
B1	W27×84	W21×55	W24×84	W30×99
B2	W21×93	W27×84	W27×84	W24×76
B3	W21×48	W18×46	W18×46	W18×55
Weight (kg)	22,006.28	20,520.36	20,663.18	**19,797.15**
Mean (kg)	23,464.25	21,039.98	22,560.24	21,171.56
Worst (kg)	25,889.75	22,972.59	24,923.44	23,054.64
SD	1315.39	776.24	1267.66	919.26

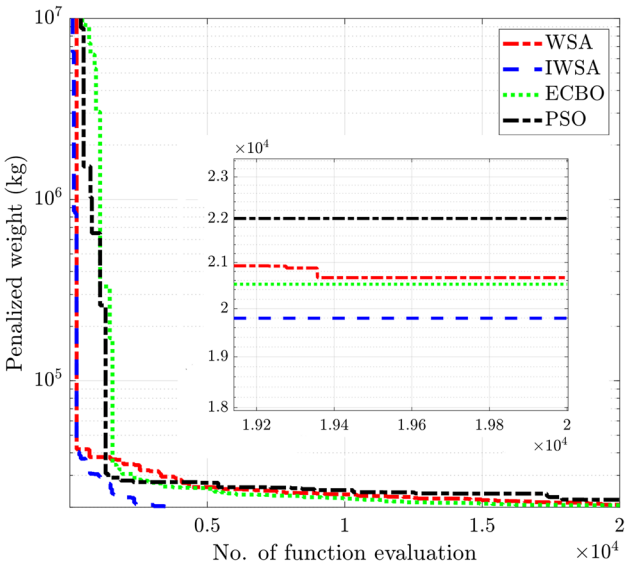

Fig. 4 Convergence history for the best design of the 6-story frame

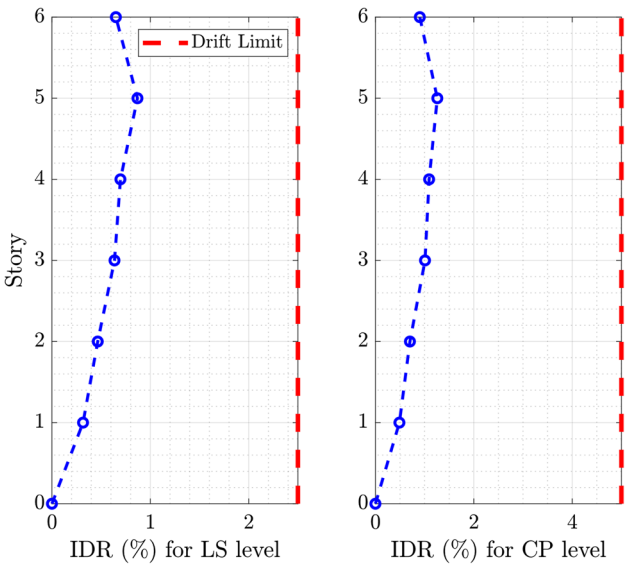

Fig. 5 Inter-story drift ratio for the best design obtained by IWSA algorithm for the 6-story frame

The IDR for the best design by IWSA is shown in Fig. 5, which shows that the final design also meets the drift ratio constraints. However, the values for the IDR of the frames are far from their allowable threshold which can be construed that this constraint has not controlled the design.

Figure 6 shows the rotation of plastic hinges for the best solution obtained for the 6-story frame (the left and the right bar plot belong to the columns and beams, respectively). In this figure, the numbering for columns and beams is started from the first story up to the last one and from left to right. For each column, the numbering begins with the lower plastic hinge and then the upper one, and for each beam, it begins with the left plastic hinge to the right one. For each plastic hinge, the existing value of the rotation is divided by the maximum allowable value of rotation ($\theta/\theta_{A.C}$) so that the values of the vertical axis are normalized for a better insight. This figure illustrates that the rotation of hinges has not exceeded the allowable values. However, this value for the CP performance level controls the designing process.

The strong column-weak beam (SCWB) criterion is checked using the following equation according to (AISC341-16 2016):

$$\frac{\sum M_{pb}}{\sum M_{pc}} \leq 1 \tag{23}$$

where $\sum M_{pb}$ denotes the sum of plastic moments in the beams projected at the centerline of the column and $\sum M_{pc}$ is the sum of plastic moments in the column below and above the joint at the intersection of the beam and column centerline. The SCWB graph for the best design is plotted in Fig. 7. In this figure, Nij denotes the j^{th} node of the i^{th} story, counting from left to right. The values for $\sum M_{pb}/\sum M_{pc}$ are directly affected by the design and classification of variables and are determined at the CP performance level. The values denoting the ratio of the leftmost nodes are slightly less than the rightmost ones; this conclusion is drawn based on the higher axial load of the right columns at CP performance level, which increases this ratio. The difference grows more noticeable as the section sizes reduce. It can be seen that in each beam-column intersection, the value of $\sum M_{pb}/\sum M_{pc}$ is less than unity, showing that this criterion is met for the best design achieved by IWSA algorithm.

7.2 12-story Frame

The second example evaluates a 4-bay, 12-story frame. The schematic of the frame, along with the groupings of columns and beams, is shown in Fig. 3b. This example is a more complex problem than the first one and consists of 24 design

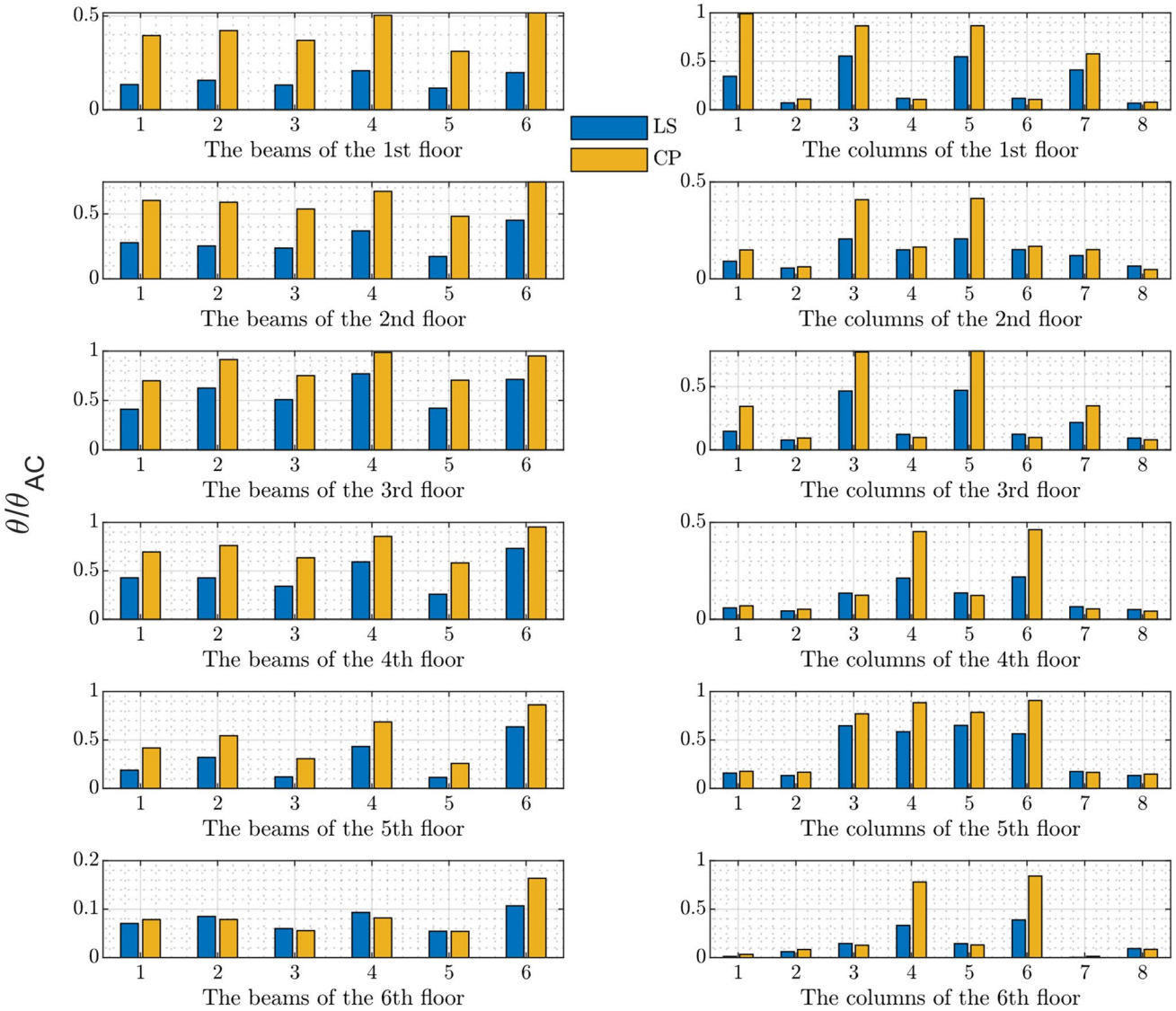

Fig. 6 Plastic hinges rotation for the best design of the 6-story frame

variables and numerous seismic constraints which makes it an arduous task for metaheuristics to converge to a feasible solution. For this example, WSA and PSO could not obtain an acceptable result without constraint violation in the six independent runs. Furthermore, since the optimization of this structure entails much more time than the first structure, and considering the outperformance of IWSA and ECBO in the previous problem, the sheer further studies of these two algorithms is justified.

Table 6 shows the best design obtained by IWSA and ECBO and the average value of the optimized weight. As shown, the best design of IWSA weighs 68,663.54 kg (bolded in the table), whereas this value for ECBO equals 77,628.72 kg. In other words, IWSA has outperformed ECBO by 11.6% in the best optimization process. In terms of the average optimized weight, Table 6 shows that IWSA has also performed better than ECBO in the six optimization runs since the mean value of IWSA is 10% less than ECBO.

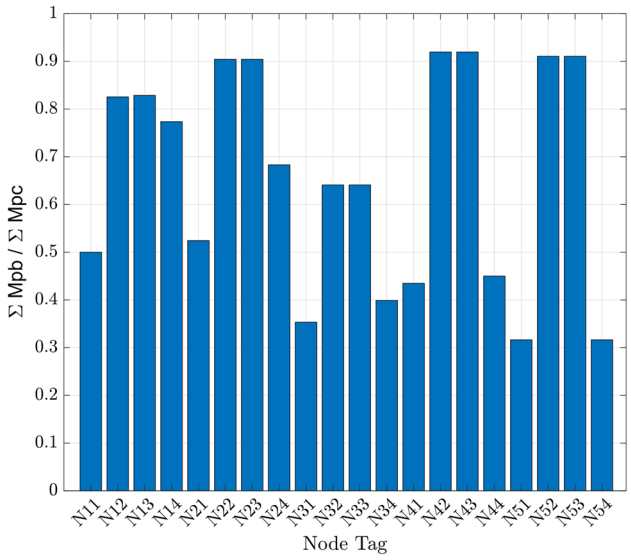

Fig. 7 Strong column-weak beam ratio plot for the best design of the 6-story frame

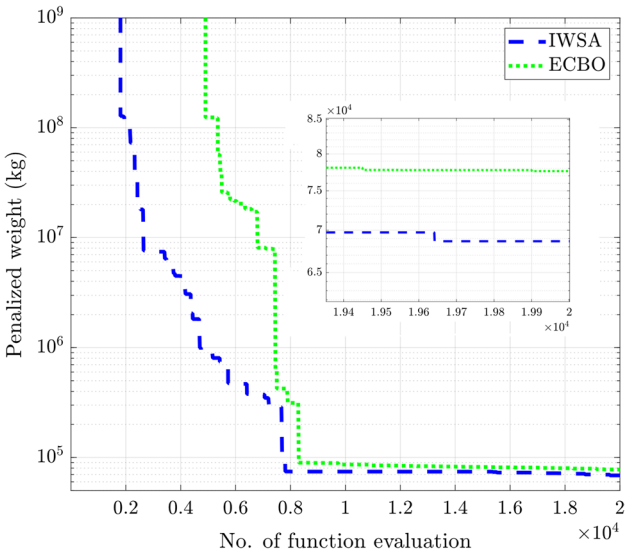

Fig. 8 Convergence history for the best design of the 12-story frame

Table 6 The best design achieved by the algorithms for the 12-story frame

Groups	ECBO	IWSA
C1	W36×260	W40×167
C2	W36×245	W27×146
C3	W30×173	W24×117
C4	W27×94	W18×97
C5	W16×77	W18×97
C6	W14×68	W12×65
C7	W40×183	W44×290
C8	W40×167	W44×290
C9	W33×387	W44×262
C10	W36×150	W18×158
C11	W36×135	W10×88
C12	W21×68	W10×68
C13	W40×199	W40×249
C14	W36×194	W36×210
C15	W36×182	W33×141
C16	W27×187	W24×117
C17	W18×97	W14×82
C18	W8×67	W10×60
B1	W24×103	W12×45
B2	W16×67	W27×102
B3	W40×167	W16×100
B4	W21×93	W18×86
B5	W14×82	W14×82
B6	W12×50	W10×54
Weight (kg)	77,628.72	**68,663.54**
Mean (kg)	83,832.74	75,484.83
Worst (kg)	90,934.18	81,320.42
SD	5571.95	4777.42

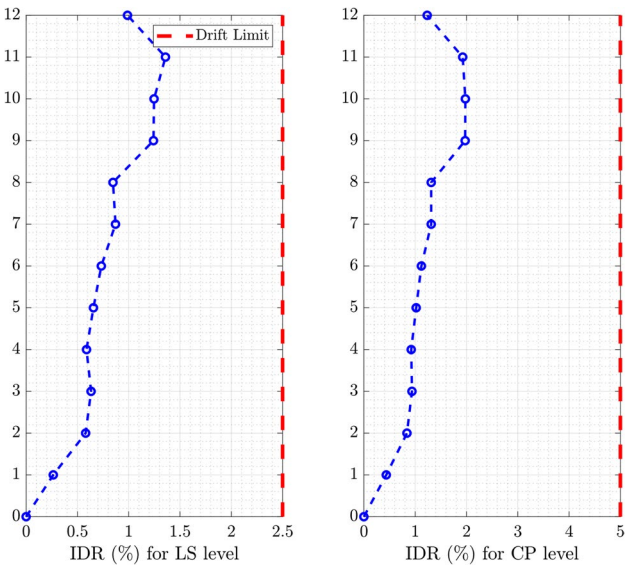

Fig. 9 Inter-story drift ratio for the best design obtained by IWSA algorithm for the 12-story frame

The best design convergence curve is depicted in Fig. 8. It is seen that IWSA has a faster convergence rate than ECBO to a large extent. For such a complex problem, a mechanism is required for an optimization algorithm to escape from the local optimum and to navigate it towards the near-optimal solution. This mechanism is designed in IWSA by the mutation of the best-so-far solution which assists it to approach the optimal solution rather than getting trapped in local optimum or searching fruitless areas of the search space.

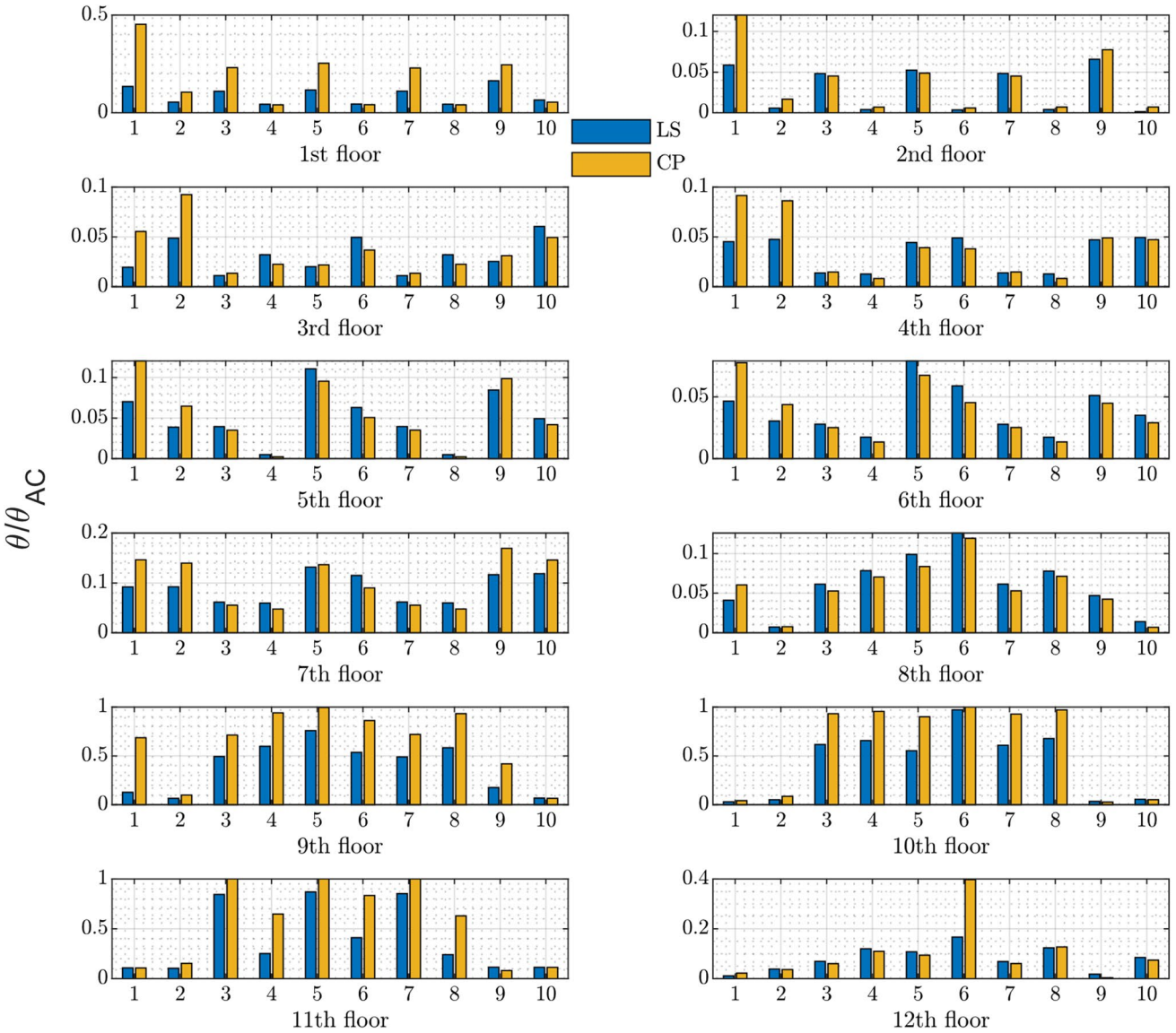

Fig. 10 Plastic hinges rotation of columns for the best design of IWSA for the 12-story frame

The IDR of the best design of the IWSA algorithm is depicted in Fig. 9, demonstrating that it has satisfied this constraint successfully.

In Figs. 10 and 11, the plastic hinge rotation of columns and beams is demonstrated. As can be seen, the orange bars (CP performance level) are near their maximum allowable values for both the columns and beams plastic hinges while for the most of the plastic hinges, the LS bars are far from their maximum allowable values. This shows that the plastic hinges rotation for the CP performance level dominates the optimization process.

In Fig. 12, the SCWB criterion is investigated for the best design of IWSA. This figure demonstrates that the SCWB criterion is satisfied for most of the nodes except a few nodes belonging to the 9th and 10th story. Since the strong column-weak beam criterion has not been explicitly taken into account as a design constraint, a few columns exhibit a ratio larger than unity. For the design of special moment frames, this criterion should be assumed as

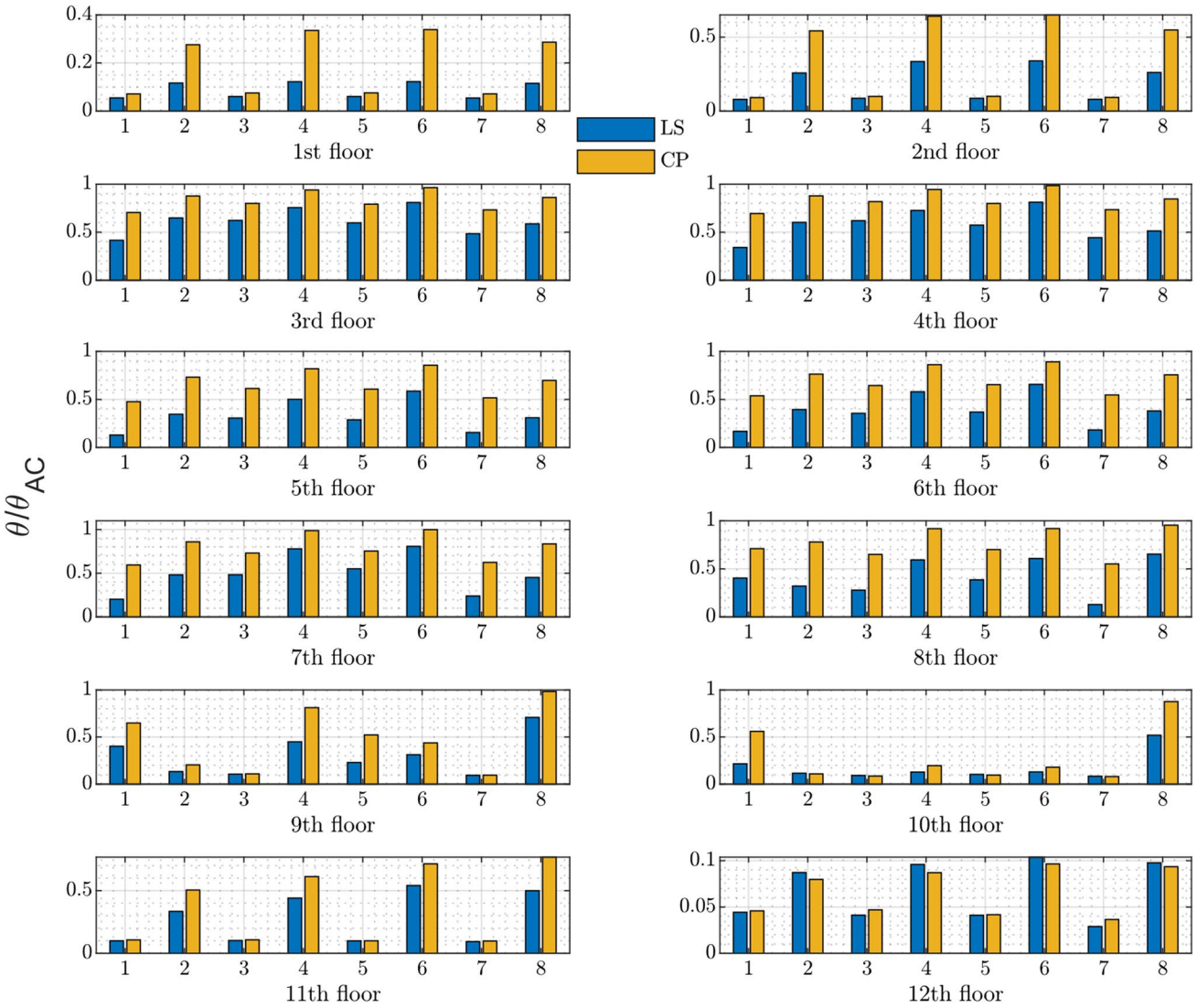

Fig. 11 Plastic hinges rotation of beams for the best design of IWSA for the 12-story frame

a constraint, and thus after achieving a final design with no violation of constraint, this criterion would also be satisfied.

7.3 Hinge Formation of the Optimal Designs

Since the CP performance-level acceptance criteria were the predominant constraints in the optimization process for the two frames considered, the distribution of the rotation of elements' endings at CP performance level is of interest to us. Figure 13 illustrates the amount of rotation ratio for each element with respect to its corresponding yield rotation, θ_y. The red circle in this figure denotes the location in which the maximum rotation ratio has occurred in either the beams or columns. By observing this figure, one can discern the critical elements in the frames which have undergone a large deformation, and the critical elements that can potentially induce soft story mechanism can be identified for prospective rehabilitation purposes.

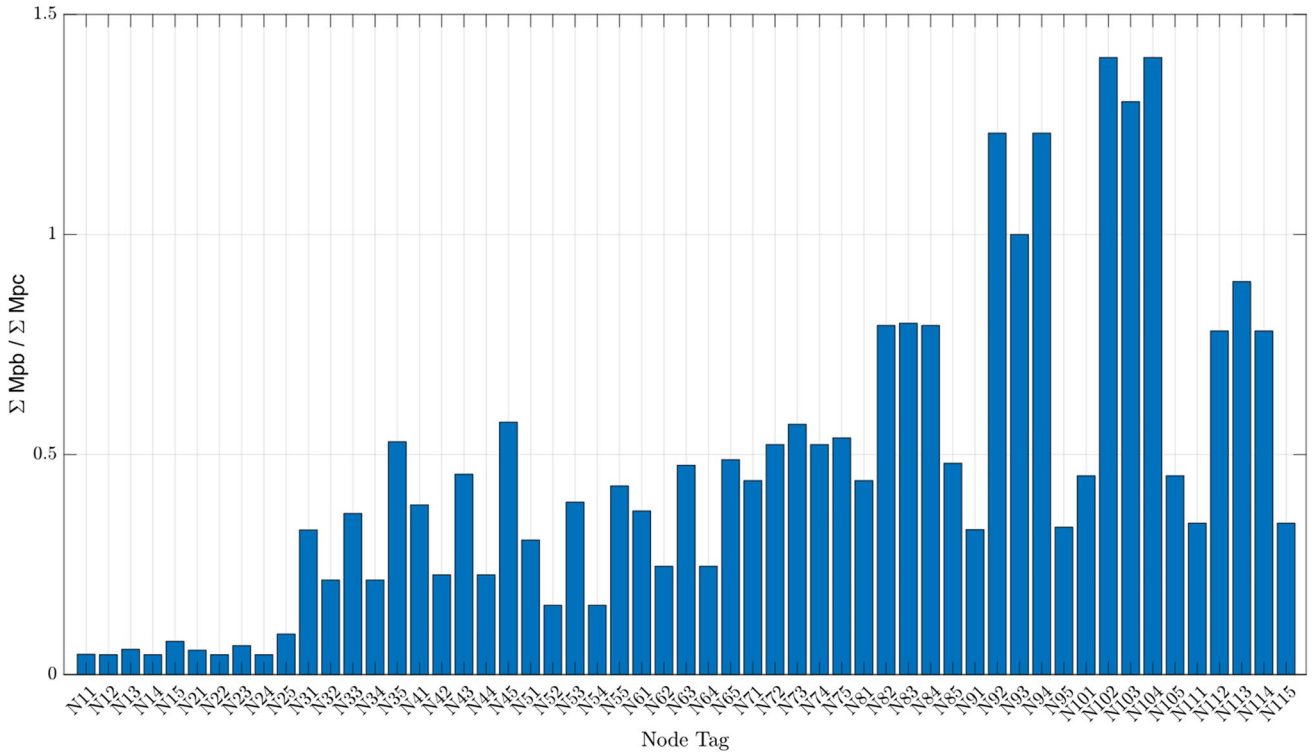

Fig.12 Strong column-weak beam ratio plot for the best design of the 12-story frame

8 Conclusion

The recently developed metaheuristic algorithm called IWSA was tested in a complex performance-based design optimization problem with system- and component-level seismic and non-seismic constraints, and the results were compared to its standard version and two other well-established metaheuristic algorithms, namely PSO and ECBO. Two MRFs were studied in this article with 9 and 24 discrete design variables for PBSDO to challenge the four algorithms and illustrate their computational performance. The following conclusions can be drawn based on the results of this paper:

- For both of the problems, the CP performance level governed the optimization process. This can be construed that while CP tends to occur in the aftermath of stronger earthquakes and less frequently than the LS performance level, the allowable damage level is so strict that its imposed design controls those of the LS performance level.
- The acceptance criteria for the plastic hinge rotation of the members at the CP performance level were the active constraint.
- The comparison of the metaheuristics shows that the IWSA algorithm is superior to its standard version and PSO in terms of accuracy of the final result as well as the required number of structural analyses.
- IWSA is competitive with one of the most successful, state-of-the-art metaheuristic algorithms, ECBO.
- An acceptable average value and standard deviation for the independent runs for the two examples clearly proved that the algorithm is also robust without sensitivity to the initial random population generated.

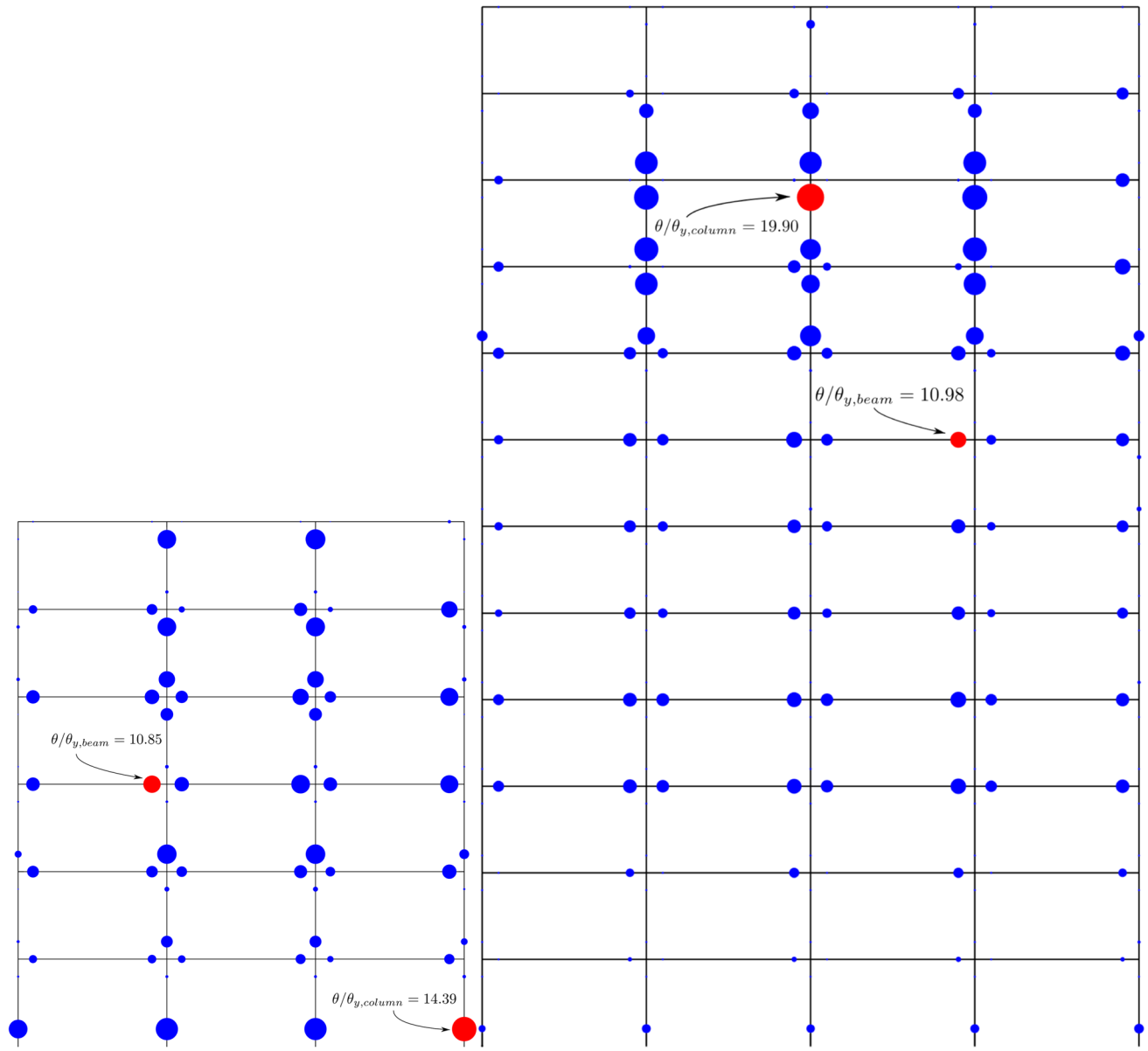

Fig. 13 Elements rotation ratios with respect to yield rotation, θ_y, for the two optimally designed frames at CP performance level (the active constraint) denoted by the blue circles; a) the 6-story frame b) the 12-story frame. The red circle shows the hinge in which the maximum rotation has occurred

- The mechanisms embedded in IWSA were useful for a successful optimization process. The GSTS as an opposition-based learning method guided the algorithm towards more promising areas of the search space, thereby increasing the convergence speed of the algorithm. The mutation technique utilized in IWSA also did a successful job in assisting IWSA to achieve a near-optimum solution, especially in the second example. Therefore, we can utilize these mechanisms in other metaheuristic algorithms to attempt to enhance their performance.

Furthermore, IWSA can also be applied in a different framework such as reliability-based design optimization (RBDO) problems, especially system reliability problems in which the failure domain involves non-convex functions with various constraints. These topics are of interest for prospective studies in this respect.

Funding No funds, grants, or other support was received.

Declarations

Conflict of interests The authors have no relevant financial or non-financial interests to disclose.

References

AISC341–16 (2016) AISC 341–16: seismic provisions for structural steel buildings. Chicago, IL: American Institute of Steel Construction (AISC)

AISC360–16 (2016) AISC 360–16: specification for structural steel buildings, American Institute of Steel Construction, Chicago, IL

ASCE41-17 (2017) ASCE Standard, ASCE/SEI, 41–17: seismic evaluation and retrofit of existing buildings. American Society of Civil Engineers, Reston, VA

ASCE7-16 (2016) Minimum design loads and associated criteria for buildings and other structures, American Society of Civil Engineers, New York

Damir S, Zeljan L, Ivan T (2021) Discrete optimization of truss structures using variable neighborhood search. Iran J Sci Technol, Transactions of Civil Engineering, 1–16.

Degertekin SO, Tutar H, Lamberti L (2020) School-based optimization for performance-based optimum seismic design of steel frames. Eng Comput. https://doi.org/10.1007/s00366-020-00993-1

Eberhart RC, Shi Y (2000) Comparing inertia weights and constriction factors in particle swarm optimization. In: Proceedings of the 2000 Congress on Evolutionary Computation. CEC00 (Cat. No.00TH8512), 16–19 July 2000.

Eftekhar Behzad, Rezaifar Omid, Karimi Mohammad Saeed (2021) A new hybrid meta-heuristic algorithm for optimum performance-based seismic designs of moment-resisting frames. Eng Optim. https://doi.org/10.1080/0305215X.2021.1907574

Fathali MA, Vaez SRH (2020) Optimum performance-based design of eccentrically braced frames. Eng Struct 202:109857. https://doi.org/10.1016/j.engstruct.2019.109857

Fathizadeh SF, Vosoughi AR, Banan MR (2021) Considering soil–structure interaction effects on performance-based design optimization of moment-resisting steel frames by an engineered cluster-based genetic algorithm. Eng Optim 53(3):440–460. https://doi.org/10.1080/0305215X.2020.1739278

FEMA-273 (1997) NEHRP guidelines for the seismic rehabilitation of buildings (FEMA 273). Federal Emergency Management Agency, Washington, DC

FEMA-356 (2000) Prestandard and commentary for the seismic rehabilitation of buildings. Federal Emergency Management Agency, Washington

FEMA-440 (2005) Improvement of nonlinear static seismic analysis procedures (FEMA-440). Federal Emergency Management Agency, Washington

Fragiadakis M, Lagaros ND (2011) An overview to structural seismic design optimisation frameworks. Comput Struct 89(11):1155–1165. https://doi.org/10.1016/j.compstruc.2010.10.021

Gholizadeh S (2015) Performance-based optimum seismic design of steel structures by a modified firefly algorithm and a new neural network. Adv Eng Softw 81:50–65. https://doi.org/10.1016/j.advengsoft.2014.11.003

Gholizadeh S, Moghadas RK (2014) Performance-based optimum design of steel frames by an improved quantum particle swarm optimization. Adv Struct Eng 17(2):143–156. https://doi.org/10.1260/1369-4332.17.2.143

Gholizadeh S, Kamyab R, Dadashi H (2013) Performance-based design optimization of steel moment frames. IUST 3(2):327–343

Gholizadeh S, Danesh M, Gheyratmand C (2020) A new Newton metaheuristic algorithm for discrete performance-based design optimization of steel moment frames. Comput Struct 234:106250. https://doi.org/10.1016/j.compstruc.2020.106250

Hasan R, Xu L, Grierson DE (2002) Push-over analysis for performance-based seismic design. Comput Struct 80(31):2483–2493. https://doi.org/10.1016/S0045-7949(02)00212-2

Hassanzadeh A, Gholizadeh S (2019) Collapse-performance-aided design optimization of steel concentrically braced frames. Eng Struct 197:109411. https://doi.org/10.1016/j.engstruct.2019.109411

Kaveh A, Dadras Eslamlou A (2020) Water strider algorithm: a new metaheuristic and applications. Structures 25:520–541. https://doi.org/10.1016/j.istruc.2020.03.033

Kaveh A, Farhadmanesh M (2019) Optimal seismic design of steel plate shear walls using metaheuristic algorithms. Period Polytech Civ Eng 63(1):1–17. https://doi.org/10.3311/PPci.12119

Kaveh A, Ilchi Ghazaan M (2014) Enhanced colliding bodies optimization for design problems with continuous and discrete variables. Adv Eng Softw 77:66–75. https://doi.org/10.1016/j.advengsoft.2014.08.003

Kaveh A, Nasrollahi A (2014) Performance-based seismic design of steel frames utilizing charged system search optimization. Appl Soft Comput 22:213–221. https://doi.org/10.1016/j.asoc.2014.05.012

Kaveh A, Farahmand Azar B, Hadidi A, Rezazadeh Sorochi F, Talatahari S (2010) Performance-based seismic design of steel frames using ant colony optimization. J Constr Steel Res 66(4):566–574. https://doi.org/10.1016/j.jcsr.2009.11.006

Kaveh A, Bakhshpoori T, Kalateh-Ahani M (2013) Optimum plastic analysis of planar frames using ant colony system and charged system search algorithms. Sci Iran 20(3):414–421. https://doi.org/10.1016/j.scient.2012.12.030

Kaveh A, Dadras A, Bakhshpoori T (2018) Improved thermal exchange optimization algorithm for optimal design of skeletal structures. Smart Struct Syst 21(3):263–278

Kaveh A, Ghazaan MI, Asadi A (2020) An improved water strider algorithm for optimal design of skeletal structures. Period Polytech Civ Eng 64(4):1284–1305. https://doi.org/10.3311/PPci.16872

Kaveh A, Ghazaan MI (2018) Meta-heuristic algorithms for optimal design of real-size structures, Springer

Kaveh A, S Malakoutirad (2010) Hybrid genetic algorithm and particle swarm optimization for the force method-based simultaneous analysis and design.

Kennedy J, Eberhart R (1995) Particle swarm optimization. In: Proceedings of ICNN'95-international conference on neural networks, 27 Nov.-1 Dec. 1995

Khalilian M, Shakib H, Basim MC (2021) On the optimal performance-based seismic design objective for steel moment resisting frames based on life cycle cost. J Build Eng 44:103091. https://doi.org/10.1016/j.jobe.2021.103091

Liu Z, Atamturktur S, Hsein Juang C (2013) Performance based robust design optimization of steel moment resisting frames. J Constr Steel Res 89:165–174. https://doi.org/10.1016/j.jcsr.2013.07.011

Makiabadi MH, Maheri MR (2021) An enhanced symbiotic organism search algorithm (ESOS) for the sizing design of pin connected structures. Iran J Sci Technol Trans Civ Eng 45(3):1371–1396

Mansouri SF, Maheri MR (2019) Performance-based seismic design of steel frames using constraint control method. Adv Struct Eng 22(12):2648–2661. https://doi.org/10.1177/1369433219849820

Mazzoni S, McKenna F, Scott MH, Fenves GL (2006) OpenSees command language manual. Pacific Earthquake Engineering Research (PEER) Center 264.

Rahnamayan S, Tizhoosh HR, Salama MMA (2008) Opposition versus randomness in soft computing techniques. Appl Soft Comput 8(2):906–918. https://doi.org/10.1016/j.asoc.2007.07.010

Saadat S, Camp CV, Pezeshk S (2014) Seismic performance-based design optimization considering direct economic loss and direct social loss. Eng Struct 76:193–201. https://doi.org/10.1016/j.engstruct.2014.07.008

Safari D, Maheri MR, Maheri A (2021) Optimum design of steel frames using different variants of differential evolution algorithm. Iran J Sci Technol Trans Civ Eng 45(4):2091–2105

Shayanfar MA, Ashoory M, Bakhshpoori T, Farhadi B (2013) Optimization of modal load pattern for pushover analysis of building structures. Struct Eng Mech 47(1):119–129

Shayanfar MA, Rakhshanimehr M, Ashoory M (2019) Adaptive load patterns versus non-adaptive load patterns for pushover analysis of building. Iran J Sci Technol Trans Civ Eng 43(1):23–36

Tizhoosh HR (2005) Opposition-Based Learning: A New Scheme For Machine Intelligence. In: International Conference on Computational Intelligence for Modelling, Control and Automation and International Conference on Intelligent Agents, Web Technologies and Internet Commerce (CIMCA-IAWTIC'06), 28–30 Nov. 2005

Wang X, Zhang Q, Qin X, Sun Y (2019) An efficient discrete optimization algorithm for performance-based design optimization of steel frames. Adv Struct Eng 23(3):411–423. https://doi.org/10.1177/1369433219872440

Zhang Y, Jin Z (2020) Quantum-behaved particle swarm optimization with generalized space transformation search. Soft Comput 24(19):14981–14997. https://doi.org/10.1007/s00500-020-04850-7